

SANDIA REPORT

SAND2012-10851

Unlimited Release

Printed December 2012

Computational Optimization of Synthetic Water Channels

David M. Rogers and Susan B. Rempé

Prepared by

Sandia National Laboratories

Albuquerque, New Mexico 87185 and Livermore, California 94550

Sandia National Laboratories is a multi-program laboratory managed and operated by Sandia Corporation, a wholly owned subsidiary of Lockheed Martin Corporation, for the U.S. Department of Energy's National Nuclear Security Administration under contract DE-AC04-94AL85000.

Approved for public release; further dissemination unlimited.

Issued by Sandia National Laboratories, operated for the United States Department of Energy by Sandia Corporation.

NOTICE: This report was prepared as an account of work sponsored by an agency of the United States Government. Neither the United States Government, nor any agency thereof, nor any of their employees, nor any of their contractors, subcontractors, or their employees, make any warranty, express or implied, or assume any legal liability or responsibility for the accuracy, completeness, or usefulness of any information, apparatus, product, or process disclosed, or represent that its use would not infringe privately owned rights. Reference herein to any specific commercial product, process, or service by trade name, trademark, manufacturer, or otherwise, does not necessarily constitute or imply its endorsement, recommendation, or favoring by the United States Government, any agency thereof, or any of their contractors or subcontractors. The views and opinions expressed herein do not necessarily state or reflect those of the United States Government, any agency thereof, or any of their contractors.

Printed in the United States of America. This report has been reproduced directly from the best available copy.

Available to DOE and DOE contractors from
U.S. Department of Energy
Office of Scientific and Technical Information
P.O. Box 62
Oak Ridge, TN 37831

Telephone: (865) 576-8401
Facsimile: (865) 576-5728
E-Mail: reports@adonis.osti.gov
Online ordering: <http://www.osti.gov/bridge>

Available to the public from
U.S. Department of Commerce
National Technical Information Service
5285 Port Royal Rd
Springfield, VA 22161

Telephone: (800) 553-6847
Facsimile: (703) 605-6900
E-Mail: orders@ntis.fedworld.gov
Online ordering: <http://www.ntis.gov/help/ordermethods.asp?loc=7-4-0#online>



Computational Optimization of Synthetic Water Channels

David M. Rogers and Susan L. B. Remppe
Sandia National Laboratories
P.O. Box 5800, Albuquerque, NM 87185-0895

Abstract

Membranes for liquid and gas separations and ion transport are critical to water purification, osmotic energy generation, fuel cells, batteries, supercapacitors, and catalysis. Often these membranes lack pore uniformity and robustness under operating conditions, which can lead to a decrease in performance. The lack of uniformity means that many pores are non-functional. Traditional membranes overcome these limitations by using thick membrane materials that impede transport and selectivity, which results in decreased performance and increased operating costs. For example, limitations in membrane performance demand high applied pressures to deionize water using reverse osmosis. In contrast, cellular membranes combine high flux and selective transport using membrane-bound protein channels operating at small pressure differences. Pore size and chemistry in the cellular channels is defined uniformly and with sub-nanometer precision through protein folding. The thickness of these cellular membranes is limited to that of the cellular membrane bilayer, about 4 nm thick, which enhances transport. Pores in the cellular membranes are robust under operating conditions in the body. Recent efforts to mimic cellular water channels for efficient water deionization produced a significant advance in membrane function. The novel biomimetic design achieved a 10-fold increase in membrane permeability to water flow compared to commercial membranes and still maintained high salt rejection. Despite this success, there is a lack of understanding about why this membrane performs so well. To address this lack of knowledge, we used high-performance computing to interrogate the structural and chemical environments experienced by water and electrolytes in the newly created biomimetic membranes. We also compared the solvation environments between the biomimetic membrane and cellular water channels. These results will help inform future efforts to optimize and tune the performance of synthetic biomimetic membranes for applications in water purification, energy, and catalysis.

Acknowledgment

We thank the LDRD office for recognizing the R&D 100 award for “Biomimetic Membranes for Water Purification” (*R&D Magazine*, 2011) and for part-time support of our Sandia postdoc, Dr. David Rogers.

Contents

1	Introduction	7
2	Approach	11
2.1	Modeling Aquaporin	11
2.2	Synthesizing a Model of the Silica Nanopore	11
2.3	Enabling Structural Analysis Methods	12
3	Results	15
3.1	Solvation and Mobility in Aquaporin and Silica Nanopores	15
4	Summary	19
	References	20

Figures

1	Biomimetic membrane pore structure resulting from growing polymer chains on a nanoporous tridymite silica surface.	12
2	Coordination environments of sodium, chloride, and water in the central pore of AQP and the biomimetic channel.	16

Tables

1	Single-ion free energies computed from free energy perturbation. Values reported in units of kcal/mol.	15
---	---	----

1 Introduction

In a recent visit to Austria, the DOE Secretary presented Sandia's biomimetic membrane technology in his talk entitled "Water Matters." The biomimetic membranes permit more efficient water purification by reverse osmosis than commercial membranes in lab-scale tests. Potentially these membranes could be optimized and adapted for commercial use in energy-efficient water desalination plants, or tuned for more efficient ion transport for energy, water purification and catalysis applications. Due to the high efficiency, biomimetic membranes can potentially save significant economic resources, thus enhancing national security. A lack of understanding about how membrane pore structure relates to membrane function, however, currently limits our ability to optimize and tune the biomimetic membranes for these important applications. The studies described here enhance our understanding of the biomimetic membranes, the cellular water channel that inspired its design, and material designs in general for efficient liquid separations and ion transport, topics important to both Water and Energy.

Modeling of the solute and solvent partitioning into membrane pores and channels, and transport processes through the pores is challenging because both of these steps require adequate representation of the long-range order of the channel environment. Biological membranes have a lower height limit of about three nanometers, and consist of an approximately two nanometer hydrophobic region sandwiched between two layers containing partially hydrated zwitterionic lipid headgroups. The aquaporin (AQP) protein spans this membrane with a bundle of alpha-helices, which make up the water binding sites in the channel and whose orientation within the membrane is influenced by the long-range membrane order. Although the reproducible amino-acid sequence and folding of aquaporin produce a regular environment for permeating chains of water molecules, variations in the overall fold of aquaporin on the order of nanoseconds may have a strong influence on averages obtained from molecular dynamics. Variations in experimental conditions also make it difficult to determine the exact number of aquaporin monomers present in synthetic lipid vesicles. This introduces experimental uncertainty in the permeability of aquaporin channels. Nevertheless, the crystal structures of aquaporin proteins facilitate modeling studies since they provide initial configurations for the molecular dynamics simulations.

Our biomimetic membranes, composed of a polymer network supported within a nanoporous silica membrane, has an even larger membrane thickness than biological membranes. By necessity, we have simulated the nanoporous membrane as thinly as possible with the expectation that bulk membrane conditions would prevail near the center of the slab. In addition to long-range ordering in the polymer layer that spans the pores, many different local environments are available within polymer-functionalized silica membranes. However, because these membranes are synthesized in bulk form, the channel density and single-channel permeability has a smaller experimental uncertainty.

Modeling of the transport process adds an additional layer of complexity onto the determination of the solute partition coefficient. Most studies to date have utilized a bulk diffusion constant model for estimating the permeability of water in polymers.[1, 2] This model is not likely to be sufficient for the restricted environment of the aquaporin or polymer channel, where transport of permeating species tend to be strongly coupled to each other. In the polymer system, we also expect that

transport will be coupled to the motion of the polymer itself, and will differ between the center and the walls of the channel. This situation requires a re-analysis of the spatial-dependence of diffusive transport from first principles. Directly computing the diffusion constant of ions within these systems is also not statistically possible due to the low counts of ions present. Instead, it will be much more computationally efficient to compute ion dynamics through simulations of forced, non-equilibrium flow, to be pursued in future work.

We endeavor to gain an enhanced understanding of the recently developed biomimetic membranes, the cellular membranes that inspire them, and the commercial desalination membranes that they outperform. We expect to publish our results in a peer-reviewed journal, which should enhance future development of efficient membranes for water and energy applications.

The key goal of the project is to further the design of new materials and the interpretation of current experimental results on our biomimetic membranes. We have made progress in accomplishing this goal through an in-depth computational examination of the chemical environment encountered by water and ions in cellular water channels that exhibit superior liquid deionization performance. The same computational study has been applied to understand the structural and chemical underpinnings of the superior performance of our new biomimetic membranes, compared to commercial analogues, and their inferior performance compared to cellular water channels.

Atomistic models have been constructed based on crystal structure data available for cellular water channels and experimental data on the biomimetic membrane pores. Molecular dynamics simulations and free energy perturbation were used to assess solvation environments and their effect on thermodynamic stability and mobility for water and ions inside the pores.

The work described here uses high performance computing resources at Sandia to create and interrogate structure versus function relationships in molecular models of cellular water channels and synthetic biomimetic membranes. Leaders in computational investigations of cellular water channels (e.g., Tajkhorshid, et al. *Science* 296:525-30, 2002) have used crystallographic structures of Aquaporin water channels to pursue molecular investigations of proton rejection mechanisms. A search of the literature reveals a lack of investigations focused on electrolyte rejection mechanisms in these channels. Our work will fill this gap in knowledge of how the cellular water channel that we wish to mimic achieves perfect rejection of ions simultaneously with fast water transport.

Although many computational studies, including our own, have focused on molecular structure-function relationships in a variety of synthetic pores (e.g., Leung, Rempe, Lorenz, *Phys. Rev. Lett.* 96:095504, 2006), none have investigated the biomimetic membrane pores. This is because the biomimetic membranes under investigation are novel in design (see the winning R&D 100 entry for Biomimetic Membranes for Water Purification on the R&D Magazine website at <http://www.rdmag.com/News/2011/06/R-D-100-2011-Winners-Announced/>).

The membranes are formed from a polypeptide deposited in molecular layers onto a coating, which lines a portion of the nanopore supporting structure composed of mesoporous silica. The active component consists of the supported polymer, or polypeptide. A novel fabrication process based on plasma-limited atomic and molecular layer deposition yields membranes nearly as thin as cellular membranes and spanning a small-diameter (2 nm) supporting pore. Measures of water

flux and deionization function compared to cycles of polymer deposition show that the polymeric biomimetic membranes fundamentally differ in structure from their commercial polymeric membrane counterparts. This new structure yields a 10-fold improvement in membrane permeability to water flow, compared to commercial membranes, while still retaining high salt rejection ratios.

Understanding why these membranes perform better than commercial desalination membranes, but not as well as cellular membranes, will enable optimization and future tuning of the membranes for other applications. These applications include membranes for fast transport of select species needed for batteries, fuel cells, supercapacitors, water purification, osmotic energy generation, and controlled catalysis.

To summarize our results, molecular modeling applied to the cellular water channels has provided insight into how these highly efficient natural channels give rise to perfect salt rejection ratios and fast water transport. Aspects of our synthetic biomimetic water channels that mimic these properties include the partially hydrophobic environment restricting the availability of water inside the channel constriction, the presence of carbonyl groups from the polyamide backbone and of hydroxyl groups from the silica surface. These studies provide the groundwork for understanding and mimicking cellular membrane channel designs.

The tight packing of polyamide chains inside our current desalination membranes has been made possible by the unique molecular layer deposition process. This dense packing has enabled us to drive out water aggregates which would otherwise solvate ions, while providing a sufficient chemical environment for water solvation and permeation. Establishing better self-organizing properties for the polymer would lead to more well-defined pore architectures and has great potential for building robust synthetic membrane analogues for a variety of applications in water and energy based on liquid separation and ion transport.

This work and its associated techniques have appeared in several published works, including summaries of ion solvation in the potassium ion channel that selectively transports potassium ions,[3] solvation of small molecules in water,[4, 5] and water and carboxylic acid solvation in the catalytic center of the carbonic anhydrase enzyme that sequesters and releases carbon dioxide.[4, 6]

2 Approach

2.1 Modeling Aquaporin

Although several reviews of aquaporin structure and function are available covering water transport,[7, 8, 9, 10] much less is known about its salt-rejecting properties. In this work, we report results on modeling the structure and free energy of ions embedded in the aquaporin water-conduction channel. In order to reduce the simulation size, correlation time, and long-range influence of the biological membrane, one out of the four symmetric conducting subunits of the aquaporin-4 structure from Ho et. al.[11] was simulated using position restraints on atoms greater than 12 Å from its central channel, and a cubic switching function energy between heights ± 14.9 to ± 16.9 Å to keep the solvent water, ions and glycerol molecules out of the membrane.

2.2 Synthesizing a Model of the Silica Nanopore

Building molecular models and generating initial structures for inhomogeneous water/silica/polymer structures can be a formidable task. We chose to employ the MMFF94 forcefield for its wide applicability to a variety of molecular functional groups and ability to handle silicon dioxide without extensive modifications.

We used a three-step process to generate the initial model. The first was cutting a 13 Å radius pore to prepare the silica nanopore's overall structure and detailed cleaning of the surface groups. We noticed that the structure of α -cristobalite was too regular, and tended to produce a few straight lines of available surface hydroxyls separated by large gaps of unavailable surface. β -cristobalite was unsuitable because the . Our final structure employed an nearly-amorphous tridymite unit cell, which was monoclinic with dimensions 9.932 by 17.216 by 81.864 Å. This was replicated to a simulation box size of 49.66 by 51.647 by 81.864 Å, followed by cutting the last axis at upper and lower planes to yield a height of 40 Å as well as cutting atoms encroaching a central, cylindrical pore. Silica atoms with less than 2 bonds were removed, while oxygens were added to make those with 3 bonds fully tetrahedral. Oxygen atoms with less than one bond were removed, and protons were added to oxygen atoms with only one bond. For the main structure investigated here, this procedure resulted in 414 surface hydroxyls, for a nominal density of 5.64 hydroxyls per square nanometer.

A second step carried out polymer functionalization by adding polymer chains of a specified length to available surface hydroxyls. This was accomplished using a library of TC (terephthaloyl chloride) and PA (para-phenylenediamine) building blocks, attached to a starting fragment of APS (aminopropyl silane). A class was built for each fragment, specifying a reference orientation with its starting atom at the origin, meant to be bonded in the positive z-direction. Each fragment also contained a specification for growing subsequent monomers using: a list of end-atoms to be deleted, the relative atom number of the atom to be built upon, a list of rotatable bonds, and an axis transformation to apply to subsequently added fragments. The initial APS fragment had

two orientations, one to be added to a single silica hydroxyl and another to be added to a pair of oxygen atoms at a distance suitable for forming two of the corners of the tetrahedral silica bonding structure. Addition of each APS fragment accordingly added three or two new hydroxyls onto which new APS molecules could be attached. Rotatable torsion angles were set randomly on each addition, and intermediate structures were validated for lack of atom-atom distances less than 0.5 as well as heavy-atom collisions closer than 1.0Å. The result of this phase of the building process is shown in Figure 1.

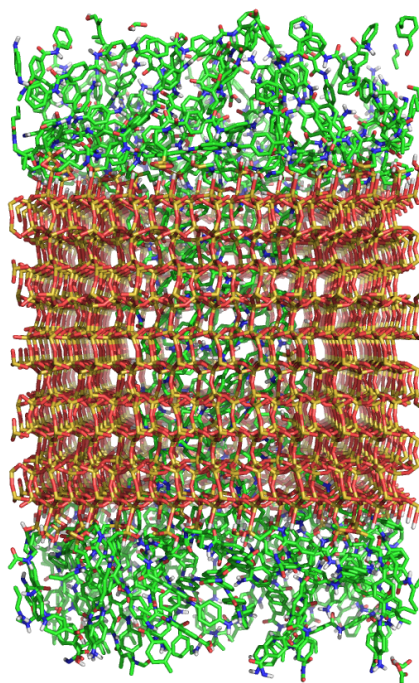


Figure 1. Biomimetic membrane pore structure resulting from growing polymer chains on a nanoporous tridymite silica surface.

The final step of the model-building process was insertion of water and ions. This was accomplished, after energy-minimizing the silica-polymer system, using the genbox program[12] with radii of 2 and 1.4Å for Si atoms and Si hydroxyl oxygens, respectively. Four waters were randomly replaced by Na⁺ and four by Cl⁻ atoms.

2.3 Enabling Structural Analysis Methods

As a part of this work, a few key computational algorithms have been built that allow unprecedented access to chemical binding structure information. The combination of a structural superposition algorithm, an extended ensemble sampling method, and a multi-state free energy method permit faster and more robust insight into binding site structural stabilities.

We developed a structural classification and clustering method that overcomes the identification problem for identical ligands. For a binding site that contains n chemically identical ligands, there are $n!$ ways to identify the molecules of a given structure with the geometry of a reference structure. This problem has factorial difficulty, and can become appreciably challenging for even $n = 6$ ligands.

To solve this problem, we implemented a routine that outputs a permutation, $\Pi_{b \rightarrow a}$ from molecules of the given structure to molecules of the reference structure. The permutations are generated by organizing matches, $b \rightarrow a$, into a product graph with n^2 nodes, each node representing a pair of allowed simultaneous matches.[13] Cliques of size n in this graph represent permutations.

The advantage of this structure is that the matching can be optimized based on superpositions of the molecules during generation of the clique. The resulting permutation should minimize the total squared-deviation

$$SD(x^0; x) = \min_{R, \Pi} \sum_{\alpha} |x_{\alpha}^0 - R \cdot x_{\Pi(\alpha)}|^2, \quad (1)$$

over all rotations, R , of the test structure in order to superimpose the test structure x onto the reference structure, x^0 .

This problem is slightly more complex than weighted clique detection, since the weight (SD) of each correspondence graph is not a simple sum of the weights attached to each node. However, the partial RMSD, summed only over the matches in a growing clique, always forms a lower bound to the total SD of the complete match. Since it is non-decreasing, it makes a suitable test for the branch-and-bound strategy employed during the clique detection algorithm. Whenever a new match pushes the total SD over the current best SD, then the presently growing clique may be abandoned. With this modification, clique detection directly outputs the minimum RMSD match.

We implemented free energy perturbation in order to compute the partition coefficients for water and ions on an absolute scale (i.e. with respect to the ligand in vacuum). In order to decrease the correlation time between samples, we exchanged Hamiltonians following the protocol of Shirts and Chodera.[14] This protocol was implemented in the NAMD2 software as well as a parallel version of a code designed for computations using the MMFF94 forcefield.

The occurrence and ligand-binding energy of each structural group forms the input to a multi-state free energy method.[15] This method was implemented in order to combine samples generated at all the intermediate coupling steps. The output of the method is a list of probability weights that are used to construct statistical averages over the binding site structures. The aggregate probability for each structure also determines a free energy of formation for that particular binding structure. Our implementation works in log-space to avoid numerical over/under-flow issues.

3 Results

3.1 Solvation and Mobility in Aquaporin and Silica Nanopores

After 2 ns of equilibration time with a time-step of 1.25 fs, a partially hydrophobic constriction just below the NPA motif (asparagine, proline, alanine) of the water channel, aquaporin 4 (AQP4), was identified for placement of water and ions for determination of the permeation free energy. This point is below the upper selectivity filter, where the pore radius is near 1.5 Å, and a small gap has formed between the water-coordinating side-chain amide of an asparagine (ASN97) and the backbone carbonyl of a histidine (HIS95) residue. The remainder of this site is made up from the hydrophobic residues isoleucine (ILE81), valine (VAL85), isoleucine (ILE96), valine (VAL100), leucine (LEU170), isoleucines (ILE174 and ILE193), and valine (VAL197), and is likely to form a free energy maximum for both permeating water and ions. Water and ions were constrained to this point using a flat-bottomed, harmonic potential (force constant 30 kJ/mol/Å²) beginning at 3 Å from the center of mass of these residues.

Env.	Na ⁺	Cl ⁻	H ₂ O
Water /Vapor Slab	-80.81(0.22)	-52.9(1.5)	0 (ref)
Polymer / Water Slab	-66.11(0.08)	-57.3(2.1)	1.65 (0.03)
AQP / Water	-69.9(0.7)	-52.2(0.5)	
Nanopore / Polymer	-66.2(0.6)	-35.8(2.1)	

Table 1. Single-ion free energies computed from free energy perturbation. Values reported in units of kcal/mol.

Table 1 presents the free energies of ion and water occupancy in the aquaporin channel computed using free energy perturbation with six equally spaced coupling parameter windows. Sodium (Na⁺) has a 10 kcal/mol free energy barrier at this location in AQP compared to water, while the free energy barrier for chloride (Cl⁻) partitioning is small due a nearly equivalent stability of chloride in water and the AQP binding site. This equivalence may suggest that AQP4 acts as a Cl⁻ channel. Although anion conductivity has been suggested for other aquaporins this conclusion has not been investigated in AQP4. Interestingly, a potassium channel called Kir4.1 is co-distributed with AQP4,[11] and both act to increase water, potassium, and chloride influx into cellular membranes at the abluminal membrane area of cerebrospinal capillaries following stimulation by vasopressin, which also up-regulates AQP4.[16]

The binding energy for Na⁺ in AQP is similar to its binding energy in the supported and unsupported polymer. This may be traced to its coordination environment, which consists primarily of carbonyl oxygens and surrounding waters in all three mediums (Fig. 2a). For Cl⁻, the picture is different. Water binds is able to bind more tightly to Cl⁻ in aquaporin. The biomimetic nanopore displays the highest Cl⁻ rejection due to a scarcity of hydrogen-bond donors and the presence of the nearby silica surface. The unsupported polymer shows a small, 3-4 kcal/mol, affinity for Cl⁻ over bulk water.

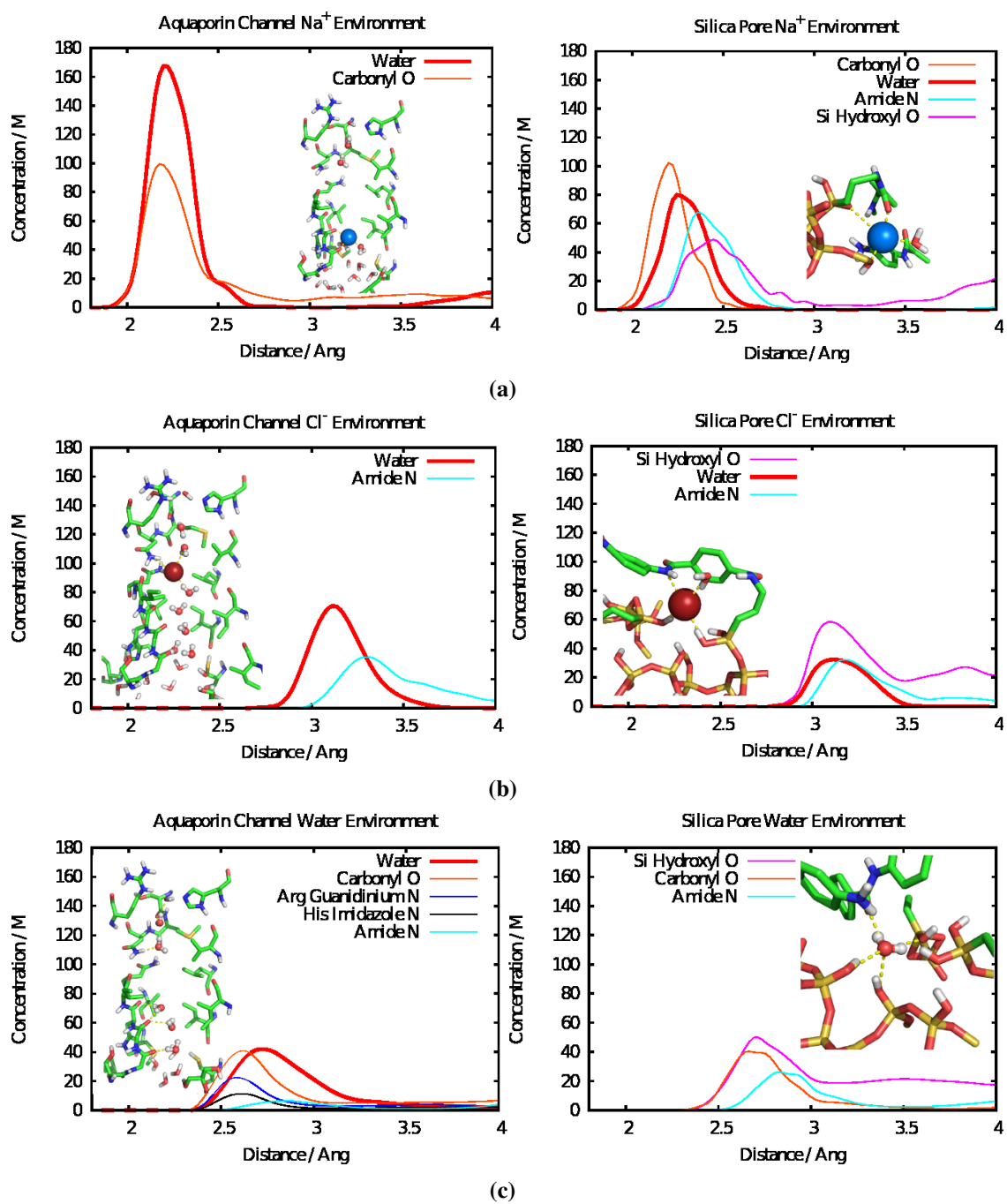


Figure 2. Coordination environments of sodium, chloride, and water in the central pore of AQP and the biomimetic channel.

The ability of these three systems to bind water makes the most interesting comparison between these three systems. In AQP, water forms a single-file chain, ordered by the regular spacing of carbonyl oxygens from the backbone of the protein alpha (α)-helices. This structure allows each water to be coordinated by two neighboring waters, aiding both binding affinity and permeability due to collective motion.

Unfortunately, this degree of ordering could not be experimentally duplicated by our polymer functionalization process. Instead, as polymers are grown layer-by-layer, the gas permeability is experimentally observed to reach a constant. This indicates that the density of polymer inside the channel has reached a maximum at this point. During this increase in density, both the water permeability and salt rejection steadily increase. We interpret these results as showing that our polymer density must reach a critical value in order to prevent formation of large pockets of water. At the critical density, water binding sites in the polymer are just close enough to form a path for water, but are sufficiently distant to prevent water aggregation.

The techniques and tools used to carry out local structural analysis of partitioning are undergoing rapid development. This report described new methods for carrying out robust structural classification that yields quantification of the binding free energy for each structure. Work is in progress to quantify short- and long-range contributions to the dielectric contribution of solvation and the spatial dependence of diffusion using all-atom molecular dynamics as well.[17]

4 Summary

We have made several scientific accomplishments during this short project focused on understanding specific chemical and structural details of ion and water solvation inside biological aquaporin channels and our synthetic biomimetic pores. A robust method for constructing computational models of polymers grafted onto silica nanopores and carrying out free energy calculations was designed, built, and tested. The free energies relate the thermodynamic stability of one ion compared to another inside the pore and provide information on ion rejection properties. New data analysis techniques were applied to large-scale numerical simulations to interrogate the structural and chemical environments experienced by water and electrolytes in the newly created biomimetic membranes. The connection we have developed between binding site chemical structures and ion/water energetics will help inform future efforts to optimize and tune the performance of synthetic biomimetic membranes for applications in water purification, energy, and catalysis.

References

- [1] M. J. Kotelyanskii, N. J. Wagner, and M. E. Paulaitis. Atomistic simulation of water and salt transport in the reverse osmosis membrane ft-30. *J. Membr. Sci.*, 139(1):1–16, 1998.
- [2] Gerhard Hummer. Position-dependent diffusion coefficients and free energies from Bayesian analysis of equilibrium and replica molecular dynamics simulations. *New J. Phys.*, 7:34, 2005.
- [3] Sameer Varma, David M. Rogers, Lawrence R. Pratt, and Susan B. Rempe. Design principles for K^+ selectivity in membrane transport. *J. Gen. Physiol.*, 137(6):479–488, 2011.
- [4] Dian Jiao and Susan B Rempe. CO_2 solvation free energy using quasi-chemical theory. *J. Chem. Phys.*, 134(22):224506–224514, 2011.
- [5] Todd M Alam, David Hart, and Susan L B Rempe. Computing the $7Li$ NMR chemical shielding of hydrated Li^+ using cluster calculations and time-averaged configurations from ab initio molecular dynamics simulations. *Physical chemistry chemical physics : PCCP*, 13(30):13629–637, 2011.
- [6] D. M. Rogers, D. Jiao, L. R. Pratt, and Rempe. Structural models and molecular thermodynamics of hydration of ions and small molecules. *Annual Reports in Computational Chemistry*, 8:71–127, 2012. invited.
- [7] J. Bernard Heymann and Andreas Engel. Aquaporins: Phylogeny, structure, and physiology of water channels. *News Physiol. Sci.*, 14(5):187–193, 1999.
- [8] Kazuyoshi Murata, Kaoru Mitsuoka, Teruhisa Hirai, Thomas Walz, Peter Agre, J. Bernard Heymann, Andreas Engel, and Yoshinori Fujiyoshi. Structural determinants of water permeation through aquaporin-1. *Nature*, 407:599–605, October 2000.
- [9] Emad Tajkhorshid, Peter Nollert, Morten ø Jensen, Larry J. W. Miercke, Joseph O’Connell, Robert M. Stroud, and Klaus Schulten. Control of the selectivity of the aquaporin water channel family by global orientational tuning. *Science*, 296(5567):525–530, April 2002.
- [10] Manish Kumar, Mariusz Grzelakowski, Julie Zilles, Mark Clark, and Wolfgang Meier. Highly permeable polymeric membranes based on the incorporation of the functional water channel protein Aquaporin Z. *PNAS*, 104(52):20719–20724, December 2007.
- [11] Joseph D. Ho, Ronald Yeh, Andrew Sandstrom, Ilya Chorny, William E. C. Harries, Rebecca A. Robbins, Larry J. W. Miercke, and Robert M. Stroud. Crystal structure of human aquaporin 4 at 1.8Å and its mechanism of conductance. *Proceedings of the National Academy of Sciences*, 106(18):7437–7442, 2009.
- [12] Berk Hess Erik Lindahl and David van der Spoel. GROMACS 3.0: A package for molecular simulation and trajectory analysis. *J. Mol. Mod.*, 7:306–317, 2001.
- [13] A. T. Brint and P. Willett. Pharmacophoric pattern matching in files of 3d chemical structures: comparison of geometric searching algorithms. *J. Mol. Graph.*, 5(1):49–56, 1987.

- [14] John D. Chodera and Michael R. Shirts. Replica exchange and expanded ensemble simulations as gibbs sampling: Simple improvements for enhanced mixing. *J. Chem. Phys.*, 135(19):194110, 2011.
- [15] Michael R. Shirts and John D. Chodera. Statistically optimal analysis of samples from multiple equilibrium states. *J. Chem. Phys.*, 129(12):124105, 2008.
- [16] M. Simard and M. Nedergaard. The neurobiology of glia in the context of water and ion homeostasis. *Neuroscience*, 129:877–896, 2004.
- [17] David M. Rogers, Thomas L. Beck, and Susan B. Rempe. An information theory approach to nonlinear, nonequilibrium thermodynamics. *J. Stat. Phys.*, 145(2):385–409, 2011.

DISTRIBUTION:

1 MS 1413	E. Ackerman, 08635
1 MS 0750	A. Halloran, 06913
1 MS 1138	S. Kuzio, 06926
1 MS 0735	J. A. Merson, 06910
1 MS 0895	S. Rempe, 08635
1 MS 0754	M. J. Rigali, 06915
1 MS 1314	D. M. Rogers, 08635
1 MS 9291	B. Simmons, 08630
1 MS 9291	M. Young, 08620
1 MS 0899	Technical Library, 9536 (electronic copy)
1 MS 0359	D. Chavez, LDRD Office, 1911

